

Kinetics of Silicate Exchange in Alkaline Aluminosilicate Solutions

Michael R. North and Thomas W. Swaddle*

Department of Chemistry, University of Calgary, Calgary, Alberta, Canada T2N 1N4

Received January 20, 2000

In strongly alkaline aqueous KOH solutions containing Si^{IV} in large excess over Al^{III} , the kinetics of exchange of monomeric silicate with small acyclic aluminosilicate solute species is much more rapid than with either cyclic aluminosilicates or any all-silicate anions. Selective inversion recovery ^{29}Si NMR studies of homogeneous solutions of stoichiometric composition 3.0 mol kg^{-1} of SiO_2 , 0.1 mol kg^{-1} of Al_2O_3 , and 8.0 mol kg^{-1} of K_2O in 60–75% D_2O gave rate constants of $2.0 \pm 0.2 \text{ kg mol}^{-1} \text{ s}^{-1}$ and $17 \pm 4 \text{ s}^{-1}$ for the forward and reverse reactions of monomeric silicate with $(\text{HO})_3\text{AlOSiO}_n(\text{OH})_{(3-n)}^{(n+1)-}$ ($n = 2$ or 3) at 0°C . These rate constants are more than 10^4 -fold faster than those extrapolated from 60 to 90°C for comparable reactions of silicate anions. The greater lability of acyclic aluminate centers relative to silicate is ascribed partly to the availability of HO– groups for condensation reactions on Al and mainly to the ease of expansion of the coordination number of Al^{III} beyond 4. The latter attribute is diminished when Al^{III} is constrained to be tetrahedral in cyclic structures. With respect to the mechanism of formation of zeolites from alkaline aqueous media, it is suggested that small, labile AlOSi units add rapidly to growing zeolitic structures “on demand”, whereas the more kinetically inert cage or ring structures cannot. This would explain why a silicate or aluminosilicate structure that is dominant among solute species *at equilibrium* in the presence of a particular cation may bear little or no geometric relation to the zeolitic framework promoted *kinetically* by that same cation.

Introduction

Aluminosilicates constitute the large majority of rock-forming minerals and consequently are not commonly thought of as being substantially water-soluble. Nevertheless, the formation of aqueous cationic complexes of the type $(\text{H}_2\text{O})_5\text{AlOSi}(\text{OH})_3^{2+}$ at low to neutral pH has biomedical,^{1,2} environmental,³ and geochemical^{4,5} implications. Furthermore, those anionic aluminosilicate species such as $(\text{HO})_3\text{AlOSiO}_n(\text{OH})_{(3-n)}^{(n+1)-}$ (species **3** in Figure 1) that can exist at least metastably in solution in relatively high concentrations at high pH^{6,7} are technologically significant, for example, in connection with the synthesis of zeolite catalysts, the exploitation of oil sands by hot water injection, scale deposition in kraft pulping, and the elimination of silicate in the Bayer process for aluminum production.^{8–10} Given that alkaline aluminate/silicate solutions containing detectable concentrations of aluminosilicate species seem to be metastable at best, it is important to learn about the kinetics of the formation and dissociation of Si–O–Al linkages. Moreover,

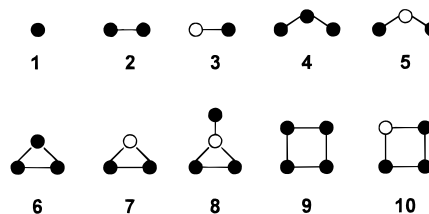


Figure 1. Representations of solute species: (●) Si centers; (○) Al centers; (–) link through an oxygen atom.

it has been noted^{11,12} that zeolites are themselves metastable so that their formation from such solutions is kinetically rather than thermodynamically controlled, and it is likely that the same is true of hydrothermal aluminosilicate transport and deposition in industrial contexts.

A previous ^{29}Si and ^{27}Al NMR study in our laboratory¹³ tentatively identified four solute species with Al–O–Si linkages (species **3**, **5**, **7**, and **10** in Figure 1) in solutions containing 1.0 mol kg^{-1} of Si^{IV} and 0.07 mol kg^{-1} of Al^{III} in 2.4 mol kg^{-1} of aqueous NaOH at 5°C . On the basis of ^{29}Si NMR line broadening, it was estimated that silicate unit exchange involving the aluminosilicate species was taking place on a time scale of around 100 ms, i.e., 10^2 – 10^3 times faster than in comparable Al-free sodium silicate solutions. Consistent with this interpretation, the limited structural information that began to emerge from quadrupolar (i.e., broad line) ^{27}Al spectra as the temperature increased was soon lost through signal coalescence.

Reconsideration of this qualitative kinetic information, however, has been made necessary by three subsequent develop-

* To whom correspondence should be addressed. Phone: (403) 220-5358. Fax: (403) 284-1372. E-mail: swaddle@ucalgary.ca

- (1) Birchall, J. D.; Bellia, J. P.; Roberts, N. B. *Coord. Chem. Rev.* **1996**, *149*, 231.
- (2) Exley, C. J. *Inorg. Biochem.* **1998**, *69*, 139.
- (3) Duan, J.; Gregory, J. J. *Inorg. Biochem.* **1998**, *69*, 193.
- (4) Gout, R.; Pokrovski, G. S.; Schott, J.; Zwick, A. J. *Solution Chem.* **1999**, *28*, 73 and references cited.
- (5) Su, C.; Harsh, J. B. *Geochim. Cosmochim. Acta* **1996**, *60*, 4275 and references cited.
- (6) Dent Glasser, L. S.; Harvey, G. J. *Chem. Soc., Chem. Commun.* **1984**, 664.
- (7) Dent Glasser, L. S.; Harvey, G. J. *Chem. Soc., Chem. Commun.* **1984**, 1250.
- (8) Swaddle, T. W.; Salerno, J.; Tregloan, P. A. *Chem. Soc. Rev.* **1994**, *23*, 319.
- (9) Gasteiger, H. A.; Frederick, W. J.; Streisel, R. C. *Ind. Eng. Chem. Res.* **1992**, *31*, 1183.
- (10) Zheng, K.; Smart, R. St. C.; Addai-Mensah, J.; Gerson, A. J. *Chem. Eng. Data* **1998**, *43*, 312.

- (11) Burkett, S. L.; Davis, M. E. In *Solid State Supramolecular Chemistry*; Alberti, G., Bein, T., Eds.; *Comprehensive Supramolecular Chemistry* 7; Elsevier: Tarrytown, NY, 1996; p 465.
- (12) Davis, M. E.; Lobo, R. F. *Chem. Mater.* **1992**, *4*, 756.
- (13) Kinrade, S. D.; Swaddle, T. W. *Inorg. Chem.* **1989**, *28*, 1952.

ments. First, it has been recognized that ^{29}Si line broadening in Al-free silicate solutions containing high alkali concentrations (which are necessary to limit the different silicate species present to a manageable number) can be induced by presumed paramagnetic impurities contained in the alkali, giving apparent Si chemical exchange rates that are much faster than the true values measured by ^{29}Si selective inversion–recovery (SIR).¹⁴ Thus, it is possible that traces of paramagnetic impurities in Al could similarly induce ^{29}Si line broadening. Second, Bell et al.^{15,16} found that line widths of aqueous silicates are influenced by ion pairing with alkali metal cations and consequently may not be reliable sources of kinetic data. Finally, Harris et al.¹⁷ have recently found that ^{27}Al resonances attributable to the simplest AlOSi solute species appear essentially immediately on mixing alkaline aluminate and silicate solutions containing a triply charged organic cation but give way slowly to lower-frequency bands characteristic of larger aluminosilicate structures. Accordingly, in an attempt to obtain definitive kinetic information, we have investigated the dynamics of silicate exchange in the smaller aluminosilicate ions in concentrated aqueous KOH using the ^{29}Si SIR technique. We chose KOH over NaOH (used in our previous aluminosilicate study¹³) because concentrated KOH aluminosilicate solutions resist gelation longer than their NaOH analogues.^{6,7}

Experimental Section

All solutions were prepared in polyethylene or Teflon–FEP containers that had been soaked successively in dilute solutions of HCl, HNO₃, and Na₂H₂EDTA prior to use. Amorphous silica was prepared by dropwise hydrolysis of freshly distilled silicon tetrachloride (Fisher, technical grade) in water. The resultant gel was dried, crushed, washed with water, and oven-dried at 250 °C. Potassium hydroxide (BDH ACS reagent grade; alternatively, Aldrich semiconductor grade, 99.99% K⁺ on metals basis excluding <0.05% Na⁺) and high-purity aluminum rod (Spex) were used as received. Stock KOH solutions were prepared by dissolving KOH pellets in freshly degassed deionized water enriched with 60–75% D₂O (Aldrich, 99.9 atom % D) and were standardized by titration with potassium hydrogen phthalate. Stock aluminate and silicate solutions were prepared by weight by dissolving aluminum rod or silica in portions of the stock KOH solutions. NMR samples were prepared by careful mixing of weighed quantities of KOH, aluminate, and silicate solutions in Teflon–FEP NMR tube liners. Because the concentrations of Si^{IV}, Al^{III}, and KOH in solution were necessarily very high and that of OH[−] was dependent on the degree of deprotonation of –OH ligands at Si centers, solution compositions are represented in terms of the formal SiO₂, Al₂O₃, and K₂O concentrations, expressed in moles per kilogram of H₂O/D₂O solvent. Dissolved oxygen was purged from the samples with Ar or N₂ before closing the NMR tube with a Teflon stopper and sealing it with Parafilm.

NMR Measurements. NMR spectra were recorded on a Bruker AMX2-300 spectrometer (59.624 MHz for ^{29}Si and 78.206 MHz for ^{27}Al) using a 10 mm probe head at a spin rate of 10 Hz. The chemical shift δ of the orthosilicate resonance (species **1**) of the ^{29}Si spectra was taken as 0 ppm. Chemical shifts of the ^{27}Al spectra were recorded relative to external aqueous Al(NO₃)₃ solution ($\delta = 0$). The aluminum present in the probe head gave a broad background signal centered at 65 ppm, which overlapped the region of interest. To correct this, a background spectrum of a sample of pure D₂O, collected using the same number of scans and the same receiver gain, was digitally subtracted from the ^{27}Al spectra of the aluminosilicate solutions.

Temperature calibrations were carried out using the proton spectra of neat ethylene glycol.¹⁸ A ^{29}Si 90° pulse width of 14.5 μs was used for experiments at −5 and +5 °C. Longitudinal relaxation times T_1 were estimated by nonselective inversion–recovery measurements (180°– τ –90°–FID– t_d), with a pulse interval of 60 s (>5 times the largest measured T_1). Selective inversion–recovery experiments were carried out by inverting the monomeric orthosilicate resonance using a DANTE sequence of 29 pulses of 1 μs with a 0.7 ms interpulse delay.

Results

The choices of solution compositions and temperature were severely restricted by a combination of factors. First, only those solutions that would remain homogeneous over at least the time scale of the NMR experiments (up to 3 days) could be considered. The dependence of the time to onset of gelation on solution composition and temperature is complex (cf. Dent Glasser and Harvey^{6,7}) and will be reported separately. In essence, long solution lifetimes are associated with high [KOH] and [Si]/[Al] of either $\gg 1$ or $\ll 1$. Second, the rather low receptivity of ^{29}Si at natural abundance required [Si] to be as high as possible such that only solutions with [Si]/[Al] $\gg 1$ could be studied in detail. Third, to keep the number of different silicate and aluminosilicate species down to a manageable few, very high alkalinities were necessary.¹⁴ Fourth, the rates of silicate exchange of the Al–O–Si species of interest turned out to be so fast that sufficiently sharp Al–O– ^{29}Si spectra could only be obtained at low [Al] and within a narrow range of temperatures low enough to retard exchange adequately but not so low to cause freezing or viscosity broadening. Viscosity broadening was evident below −5 °C, whereas above +5 °C the exchange-broadened signals from the more labile species overlapped excessively or coalesced.

Silicon-29 line widths at half peak height ($\Delta\nu_{1/2}$) for [Si]/[Al] = 4:1 to 22:1 are summarized in the Supporting Information (Table S1). For [Si]/[Al] = 1:1 ([Si] = [Al] = 0.3 mol kg^{−1}, [K₂O] = 8.0 mol kg^{−1}) at 8 °C, the ^{29}Si signals of the species **2**, **7**, and **8** coalesced with $\Delta\nu_{1/2} = 22$ Hz, and that of the key aluminosilicate **3** was so strongly broadened as to be unobservable. These observations gave strong qualitative confirmation of the lability of Al–O–Si links relative to Si–O–Si in small aluminosilicate species (cf. Bell et al.¹⁹) but at the same time limited the options to measure silicate exchange rate constants to two solution compositions with [Si]/[Al] nominally 10:1 and 15:1 ([Al₂O₃] = 0.10 mol kg^{−1} and [K₂O] = 8.0 mol kg^{−1}) and a temperature range of about −5 to +5 °C. The 15:1 solution was duplicated using different sources of solutes, notably KOH of certified low content of metal ions other than K⁺ (Aldrich semiconductor grade); as noted below, the duplicate solutions gave essentially the same results except that ^{29}Si T_1 values for the higher purity KOH were about 17% longer on the average.

Figure 2 shows how the low-temperature ^{29}Si NMR spectrum of a solution containing 2.0 or 3.0 mol kg^{−1} of SiO₂ and 8.0 mol kg^{−1} of K₂O (BDH) was changed by the introduction of minor concentrations of Al^{III} (the 10:1 and 15:1 solutions). New peaks ascribed to aluminosilicate species **3**, **5**, and **8** emerged, and that assigned to the silicate dimer (species **2**) was substantially reduced in height relative to the cyclic silicate trimer **6**. Assignments of the ^{29}Si resonances were made according to the principles previously established, bearing in mind that ^{29}Si chemical shifts relative to the aqueous silicate

(14) Vallazza, E.; Bain, A. D.; Swaddle, T. W. *Can. J. Chem.* **1998**, *76*, 183.

(15) McCormick, A. V.; Bell, A. T.; Radke, C. J. *J. Phys. Chem.* **1989**, *93*, 1733.

(16) Hendricks, W. M.; Bell, A. T.; Radke, C. J. *J. Phys. Chem.* **1991**, *95*, 9513.

(17) Harris, R. K.; Parkinson, J.; Samadi-Maybodi, A.; Smith, W. *Chem. Commun.* **1996**, 593.

(18) Ammann, C.; Meyer, P.; Merbach, A. E. *J. Magn. Reson.* **1982**, *46*, 319.

(19) Mortlock, R. F.; Bell, A. T.; Radke, C. J. *J. Phys. Chem.* **1991**, *95*, 372.

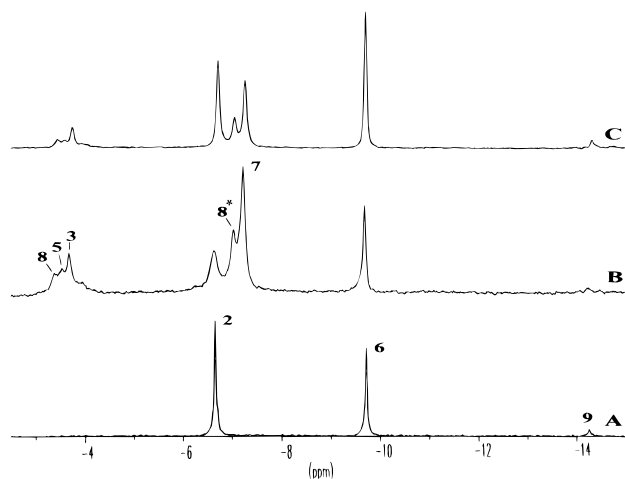


Figure 2. ^{29}Si spectra of silicate solutions at $-9\text{ }^\circ\text{C}$ (chemical shifts relative to the strong monomeric silicate resonance at 0 ppm, not shown) in the presence and absence of minor concentrations of Al: (A) 8.0 mol kg^{-1} of K_2O (BDH) and 2.0 mol kg^{-1} of SiO_2 ; (B) as in (A) but with 0.10 mol kg^{-1} of Al_2O_3 ($[\text{Si}]/[\text{Al}] = 10:1$); (C) 8.0 mol kg^{-1} of K_2O (BDH), 3.0 mol kg^{-1} of SiO_2 , and 0.10 mol kg^{-1} of Al_2O_3 ($[\text{Si}]/[\text{Al}] = 15:1$). For ease of comparison, the vertical scales are arbitrarily chosen. 8^* denotes the intracyclic Si sites of species **8**.

monomer are cation-, pH-, and solvent-dependent.^{13,19–22} Thus, the new features near -4 ppm represent terminal SiO_4 units attached to one Al center, and those near -7 ppm correspond to SiO_4 centers linked to one Al and one Si.

Aluminum-27 spectra (Supporting Information, Figure S1) for solutions with $[\text{Si}]/[\text{Al}] = 10:1$ and $15:1$ relative to Si-free $\text{Al}(\text{OH})_4^-$ (all with 8.0 mol kg^{-1} of K_2O) showed that no significant concentrations of free $\text{Al}(\text{OH})_4^-$ existed in the former solutions and implied that the main AlOSi species present contained Al centers with either one or two $-\text{OSi}$ links (the latter predominating at $[\text{Si}]/[\text{Al}] = 15:1$). Consequently, the attack of $\text{Al}(\text{OH})_4^-$ on various silicate species can be disregarded as a mechanism of silicate exchange in aluminosilicate species in our experiments; in particular, the exchange of Si in species **3** as observed by ^{29}Si SIR does not involve dynamic equilibrium with $\text{Al}(\text{OH})_4^-$ and **1** to any appreciable extent.

The ^{29}Si peak heights of all silicate species other than **1** are expected to decrease as the temperature increases because of the shift of equilibrium populations toward the monomer,²² but Figure 3 shows that exchange broadening also contributes to the diminution of peak heights for several species, most notably **1**. There is marked line broadening of the silicate monomer resonance even at subambient temperatures, in contrast to the minimal temperature effects on ^{29}Si line widths seen in this temperature range in highly alkaline Al-free silicate solutions.^{13,14,23} In contrast, the line widths of the cyclic Si_3 species **6** at -9.7 ppm and the cyclic Si_4 species **9** at -14.3 ppm are effectively independent of temperature, -5 to $+75\text{ }^\circ\text{C}$. This implies that species **1** is involved in rapid exchange with Al-containing species under these conditions, but **6** and **9** are not. In effect, then, the addition of a small amount of aluminate catalyzes silicate exchange reactions in *acyclic* species. Above ambient temperatures, the ^{29}Si resonances attributed to Si bound to Al atoms disappear because of exchange broadening; thus,

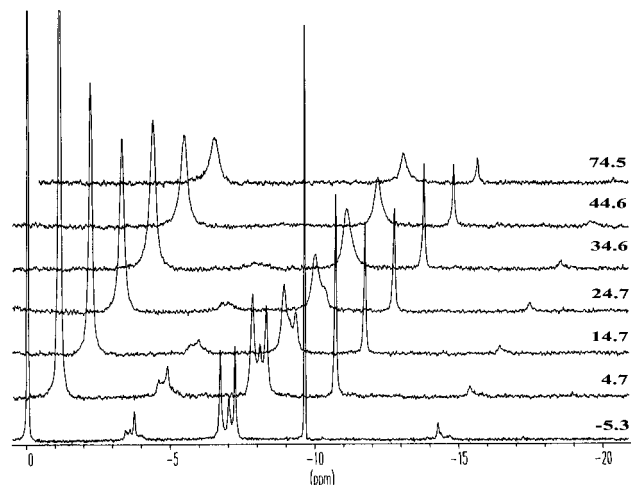


Figure 3. Temperature dependence of the ^{29}Si NMR spectrum of a solution with $[\text{Si}]/[\text{Al}] = 15:1$ (solution (C) of Figure 2). Vertical scale is the same for all temperatures (the silicate monomer peak at 0 ppm is truncated at the two lowest temperatures).

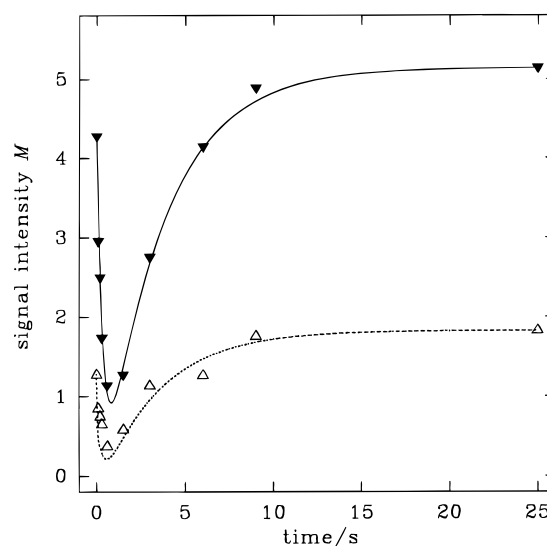


Figure 4. Evolution of ^{29}Si peak heights (relative to silicate monomer **1** = 100) of species **3** (\blacktriangledown) and **5** (\triangle) following selective inversion of **1** at $4.7\text{ }^\circ\text{C}$ in a solution containing 8.0 mol kg^{-1} of K_2O (Aldrich), 3.0 mol kg^{-1} of SiO_2 , and 0.10 mol kg^{-1} of Al_2O_3 ($[\text{Si}]/[\text{Al}] = 15:1$). Curves correspond to $k_1' = 0.055\text{ s}^{-1}$, and $T_{1(i)}$ values are as in Table 1.

SIR experiments involving aluminosilicate species were limited to the temperature regime -5 to $+5\text{ }^\circ\text{C}$.

Selective inversion of the ^{29}Si signal of species **1** in the 10:1 and 15:1 solutions at -5 and $+5\text{ }^\circ\text{C}$ showed that its magnetization M_1 was transferred on a time scale of less than 1 s (cf. $T_1 \approx 3\text{--}5\text{ s}$) to the ^{29}Si resonances of species **3** and **5** (Figure 4) but not to the Si sites of species **7** or the intracyclic Si of species **8** in this time regime (Supporting Information, Figure S2). A barely discernible time dependence of the extracyclic Si resonance intensity of species **8** paralleled that of species **5** and was attributed to overlap with the latter band rather than to silicate exchange on **8**. As anticipated,¹⁴ no ^{29}Si exchange was detectable at these low temperatures for the Al-free species **2**, **6**, and **9** (Figure S2). Consequently, the SIR results can be modeled on the basis of just one chemical exchange process:



(20) Mortlock, R. F.; Bell, A. T.; Chakraborty, A. K.; Radke, C. J. *J. Phys. Chem.* **1991**, *95*, 4501.

(21) Mortlock, R. F.; Bell, A. T.; Radke, C. J. *J. Phys. Chem.* **1991**, *95*, 7847.

(22) Kinrade, S. D.; Swaddle, T. W. *Inorg. Chem.* **1988**, *27*, 4253.

(23) Kinrade, S. D.; Swaddle, T. W. *Inorg. Chem.* **1988**, *27*, 4259.

Because ^{29}Si SIR measurements could only be made with $[\text{Si}] \gg [\text{Al}]$, the population of ^{29}Si sites of species **1** greatly exceeded those of **3** and **5** such that signals due to the latter two species were relatively very weak and the effect of chemical exchange on the ^{29}Si magnetization of **1** was much less evident than on those of **3** and **5**. Furthermore, as Figure 2 shows, ^{29}Si signals due to species **3**, **5**, and the side group of **8** overlapped to some extent such that the corresponding peak areas, which are the true measures of magnetization and concentration, could not be accurately measured even with a curve-fitting routine. Consequently, peak heights for species i were taken in lieu of areas as approximate measures of the magnetizations M_i , since overlap under the peak maxima was unimportant. The peak heights would have been somewhat reduced by chemical exchange line broadening, but this effect was minimal because adequate resolution of these peaks was only obtainable at relatively slow rates of chemical exchange in the first place. In any event, peak heights were found to correspond satisfactorily to peak areas, however rough the latter.

For the purpose of analysis of the SIR data using the Bain–McClung CIFIT program,¹⁴ the concentration of the silicate monomer **1** was equated with its equilibrium magnetization M_1^∞ represented as 100 arbitrary units. The CIFIT analysis then gives a pseudo-first-order forward rate constant $k_1' = k_1[\text{1}]/100$ for process 1, and the equilibrium mass-law relation allows elimination of the corresponding reverse rate constant k_{-1}' ,

$$k_{-1}' = 2M_1^\infty M_3^\infty k_1' / M_5^\infty \quad (2)$$

such that the kinetic matrix¹⁴ describing the evolution of M_i as a function of the delay times t can be written as

$$\frac{d}{dt} \begin{bmatrix} M_1 \\ M_3 \\ M_5 \end{bmatrix} = k_1' \begin{bmatrix} -M_3^\infty & 0 & M_1^\infty M_3^\infty / M_5^\infty \\ 0 & -M_1^\infty & M_1^\infty M_3^\infty / M_5^\infty \\ M_3^\infty & M_1^\infty & -2M_1^\infty M_3^\infty / M_5^\infty \end{bmatrix} \begin{bmatrix} M_1 \\ M_3 \\ M_5 \end{bmatrix} \quad (3)$$

Values of M_i for the 15:1 solutions at -5 and $+5$ °C, and the 10:1 solution at -5 °C, were fitted to the delay times using the CIFIT program.¹⁴ The program calculates “best” values of k_1' , $T_{1(i)}$, M_i^∞ , and the initial M_i^0 by minimizing the total of all least-squares residuals, but in the present study this sum was heavily dominated by contributions from the relatively intense M_1 such that the resulting fit of the kinetically informative M_3 and M_5 data was often unrealistic if all the parameters were allowed to vary, either all at once or in sets. Fortunately, all the $T_{1(i)}$ values could be separately measured by a nonselective inversion–recovery pulse sequence with standard errors of less than 1%, so these quantities were determined independently and introduced as fixed parameters in the CIFIT analysis. Furthermore, the measured values of M_3^0 , M_5^0 , M_3^∞ , and M_5^∞ were not found to be significantly improved by the fitting process, and they were also fixed in the final computations. Thus, the final analysis was carried out by allowing the program to recalculate M_1^0 and M_1^∞ values for series of chosen values of k_1' ; the value of k_1' that gave the best visual fit of the M_3 and M_5 data (exemplified by Figure 4) was adopted. The recalculated M_1^0 and M_1^∞ values agreed well (less than $\pm 2\%$) with those directly measured. The precision in the k_1' values obtained by visual fitting was $\pm 15\%$ or better. The adopted parameters summarized in Table 1 gave excellent fits of the M_1 data as exemplified by Figure S2, which also shows that there was no significant transfer of magnetization from **1** to the ^{29}Si signals of species **2**, **7**, and **8** while M_1 evolved.

Table 1. Solution Compositions, ^{29}Si Longitudinal Relaxation Times, and Silicate Exchange Rate Constants

	[Si]/[Al] (nominal)				
	10:1	15:1	15:1	15:1	15:1
temp/°C	−5.3	−5.3	−5.3	4.7	4.7
[K ₂ O]/mol kg ^{−1}	8.0 ^a	8.0 ^a	8.0 ^b	8.0 ^a	8.0 ^b
[Al] = 2[Al ₂ O ₃]/mol kg ^{−1}	0.199	0.197	0.204	0.197	0.204
[Si] = [SiO ₂]/mol kg ^{−1}	2.01	3.03	3.06	3.03	3.06
[OH [−]] ≈ 2[K ₂ O] _{net} /mol kg ^{−1} ^c	11.8	9.7	9.7	9.7	9.7
[1]/mol kg ^{−1}	1.15	1.58	1.50	1.56	1.56
[3]/mol kg ^{−1}	0.093	0.073	0.068	0.082	0.080
[5]/mol kg ^{−1}	0.026	0.015	0.012	0.019	0.011
<i>K</i> /kg mol ^{−1}	0.24	0.13	0.12	0.15	0.11
$T_{1(1)}$ /s ^{−1}	0.35	0.33	0.28	0.36	0.30
$T_{1(3)}$ /s ^{−1}	0.29	0.24	0.21	0.31	0.28
$T_{1(5)}$ /s ^{−1}	0.27	0.25	0.21	0.38	0.32
k_1' /s ^{−1}	0.020	0.018	0.018	0.045	0.055
k_1 /kg mol ^{−1} s ^{−1}	1.7	1.1	1.2	2.9	3.5
k_{-1} /s ^{−1}	7.1	9	10	20	31

^a From BDH ACS reagent grade KOH; in addition, 0.13 mol kg^{−1} of K₂CO₃ was present. ^b From Aldrich semiconductor grade KOH; in addition, 0.18 mol kg^{−1} of K₂CO₃ was present. ^c Nominal concentration, calculated assuming all Al was present as “KAlO₂” and all Si as “K₂SiO₃”, taking no account of polymerization and partial protonation of the silicate ions.

The true molal concentration of **1** was calculated by multiplying the stoichiometric [SiO₂] by the integrated area of the ^{29}Si NMR signal of the monomer and dividing by the total of the integrated areas of all ^{29}Si solute resonances. Values of k_1' generated by the CIFIT program were then multiplied by 100/[1] to give k_1 in kg mol^{−1} s^{−1}; these units were chosen rather than the traditional L mol^{−1} s^{−1} because of the need to define conditions in such concentrated solutions in terms of the amount of each component present. The concentrations of the exchange-active species **3** and **5** were calculated from [1] using the ^{29}Si peak heights (halved, in the case of **5**) relative to **1**, whence the equilibrium constant K for process 1 was calculated as [5]/[1][3]. Values of k_1 , k_{-1} , and K for the 15:1 solutions were not significantly dependent upon the sources and purities of the reagents used but were not quite the same for the 10:1 solutions. The latter observation is as expected because of differences in [OH[−]] and in the activity of solvent water (which was probably substantially less than unity). The values of T_1 in Table 1, however, are about 17% shorter on the average for solutions made up with BDH ACS reagent grade KOH than for those made with Aldrich semiconductor-grade KOH, which is especially low in metals other than K and Na. This confirms that any but the purest alkali can contain levels of trace paramagnetics high enough to influence ^{29}Si relaxation processes at high pH and hence to throw doubt on any attempt to extract chemical exchange rate constants from ^{29}Si line widths alone.¹⁴

An attempt to determine k_1 using estimated peak areas gave slightly higher apparent rate constants because of band overlap involving species **3** and **5**, but these computations served to increase confidence in the k_1 values obtained from peak heights.

Discussion

It is qualitatively obvious, from the lack of any detectable magnetization transfer from the silicate monomer to any all-silicate species (e.g., to species **2**, Figure S2) under the conditions of these experiments, that process 1 is very much faster than ^{29}Si exchange between silicate species. Furthermore, Vallazza et al.¹⁴ found that for silicates in aqueous KOH solutions without Al temperatures of about 90 °C were necessary to observe ^{29}Si exchange rates comparable to those reported here for aluminosilicate species at -5 and $+5$ °C.

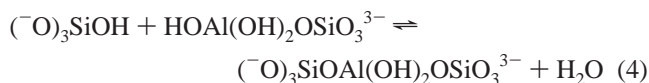
Table 2. Comparison of Estimated Rate and Equilibrium Constants for Silicate Exchange on Small Silicate and Aluminosilicate Anions in Aqueous KOH at 0 °C

process	$k_{\text{forward}}/\text{kg mol}^{-1} \text{ s}^{-1}$	$k_{\text{reverse}}/\text{s}^{-1}$	$K/\text{kg mol}^{-1}$
1 + 3 → 5 ^a	2.0 ± 0.2	17 ± 4	0.12 ± 0.02
1 + 1 → 2 ^b	7 × 10 ⁻⁵	7 × 10 ⁻⁴	0.10
1 + 2 → 6 ^b	1.1 × 10 ⁻⁵	2.3 × 10 ⁻⁵	0.48

^a Interpolated data, this work; [SiO₂] = 3.0 mol kg⁻¹, [Al₂O₃] = 0.1 mol kg⁻¹, [K₂O] = 8.0 mol kg⁻¹. ^b Extrapolated from data of ref 14; [SiO₂] = 2.8 mol kg⁻¹, Al absent, [K₂O] = 6.5 mol kg⁻¹.

On the other hand, *quantitative* comparison of the rates of ²⁹Si exchange of aluminosilicate and silicate analogues is difficult because rate constants must be extrapolated over a wide temperature range, whereas measurements of k_1 and k_{-1} for process 1 are available only for two temperatures 10 °C apart and are subject to uncertainties of up to ±20%. Fortunately, more precise ²⁹Si exchange data for all-silicate systems are available over a 30 °C range.¹⁴ Accordingly, in Table 2, averaged values of k_1 (more generally called k_{forward}), k_{-1} (k_{reverse}), and K ($=k_{\text{forward}}/k_{\text{reverse}}$) for process 1 are interpolated to the mid-range reference temperature of 0 °C and compared with corresponding parameters for some silicate–silicate exchanges extrapolated from 60 to 90 °C.¹⁴ It should be noted that the all-silicate processes were studied¹⁴ in a less strongly alkaline solution than the silicate–aluminosilicate exchange; consequently, since OH⁻ retards silicate–silicate exchanges,²³ the latter are even slower relative to process 1 than the data of Table 2 suggest. The exact all-Si analogue of process 1 would be the formation of species **4** from **1 + 2**, but the rate of the latter exchange was not accurately measurable¹⁴ because of signal overlap problems and cyclization of **4** to **6**, and rate data are available only for the overall equilibrium between **6** and **1 + 2**. However, process 1 may be reasonably compared to the dimerization of the silicate monomer. Seen in this light, and given the difference in [OH⁻] between the data sets, the data of Table 2 show that silicate exchange at an Al center is *at least* (2 × 10⁴)-fold faster than at a comparable Si center at 0 °C.

At the very high pH values (~15) and relatively low Al concentrations of our experiments, any free Al monomer is expected to be in the form Al(OH)₄⁻, with possible trace amounts of Al(OH)₆³⁻.²⁴ Raman spectra of *concentrated* aqueous aluminates²⁵ and ²⁷Al NMR of solids from freeze-dried *partly acidified* aluminate solutions²⁶ suggest that more complex aluminate species might be present in water under certain conditions, but these observations serve to confirm that tetrahedral Al species were strongly dominant and that no Al–O⁻ functions were present at the high pH and fairly low [Al] of our experiments. On the other hand, the first and second pK_a values of the isoelectronic Si(OH)₄ are 9.47 and 12.65, respectively,²⁷ and the third pK_a may be estimated to be 15–16 so that in our experiments monomeric silicate would be present as a mixture of (HO)₂SiO₂²⁻ and HOSiO₃³⁻. The formation of both silicate polymers and aluminosilicates is essentially a condensation (water elimination) process, for example,



(24) Akitt, J. W. *Prog. Nucl. Magn. Reson. Spectrosc.* **1989**, *21*, 1.

(25) Molenaar, R. J.; Evans, J. C.; McKeever, L. D. *J. Phys. Chem.* **1970**, *74*, 3629.

(26) Bradley, S. M.; Hanna, J. V. *J. Am. Chem. Soc.* **1994**, *116*, 7771.

(27) Svensson, I. L.; Sjöberg, S.; Öhman, L.-O. *J. Chem. Soc., Faraday Trans. 1* **1986**, *82*, 3635.

The greater lability associated with Al centers relative to Si may therefore be ascribed in part to the greater availability of the protons necessary for process 4 on the Al oxygens.²⁸ It may also be that the detailed mechanism involves nucleophilic attack of an –O⁻ function of the silicate monomer on an Al or Si center, leading to expulsion of OH⁻, in which case the relative lability of Al centers may reflect their greater propensity for expanding their oxygen coordination number beyond 4.

The latter possibility would explain why small aqueous aluminosilicate species are very labile in silicate exchange, whereas aluminosilicate entities in which the Al is part of a ring or cage structure are not.¹⁷ The simplest examples of cyclic aluminosilicates are the species **7** and **8**, in which the coordination of the Al atom is constrained to remain tetrahedral by virtue of the Al being part of an AlSi₂O₃ ring. Indeed, we find that the Si centers inside both rings (and probably also the silicate side-group in **8**) do not exchange measurably with monomeric silicate on a time scale on which Si exchange among species **1**, **3**, and **5** is rapid.

The observed lability of small aluminosilicate anions such as **3** and **5** and the relative inertness of larger cage or ring species¹⁷ may explain why the structures of the latter solutes do not seem to relate directly to those of zeolites formed from alkaline aluminate/silicate solutions containing them, even though there is general agreement that zeolite formation from aluminosilicate gels is solution-mediated (at least in part).^{8,11} Knight, in particular, has argued that the traditional concept of secondary building units (i.e., aluminosilicate cage and ring solute species with structural features anticipating those of the zeolite) in zeolite formation is unsupported.²⁹ However, small, labile AIO_{Si} units should be able to add rapidly to growing zeolitic structures (either actual zeolite crystals or locally formed polymeric precursors¹¹) “on demand”, whereas the more kinetically inert cage or ring structures cannot. The detailed mechanism of addition of small AIO_{Si} units to the zeolite structure or its precursor is presumably orchestrated by the cations present (alkali metal, tetraalkylammonium, etc.) in a manner quite different from the cation–anion interactions that stabilize particular equilibrium distributions of silicate rings and cages in solution.^{30,31} Thus, a silicate or aluminosilicate structure that is dominant among solute species *at equilibrium* in the presence of a particular cation may bear little or no geometric relation to the zeolitic framework promoted *mechanistically* by that same cation. In other words, this is an example of the interplay of *thermodynamic* versus *kinetic* control of the course of chemical reactions.

Acknowledgment. We thank the Natural Sciences and Engineering Research Council of Canada for financial support.

Supporting Information Available: Listing of ²⁹Si NMR line widths for various [Si]/[Al] ratios, ²⁷Al NMR spectra in the presence and absence of Si, evolution of ²⁹Si magnetization of species **1**, **2**, **7**, and **8** following selective inversion of **1**. This material is available free of charge via the Internet at <http://pubs.acs.org>.

IC0000707

(28) A reviewer has kindly pointed out that the signal of species **6** broadens much less than those of **1** and **2** as the temperature is increased in *Al-free* solutions as well, suggesting that the kinetic inertness of silicate rings at very high pH is due to their lack of protons.

(29) Knight, C. T. G. *Zeolites* **1990**, *10*, 140.

(30) Kinrade, S. D.; Knight, C. T. G.; Pole, D.; Syvitski, R. T. *Inorg. Chem.* **1998**, *37*, 4272.

(31) Kinrade, S. D.; Knight, C. T. G.; Pole, D.; Syvitski, R. T. *Inorg. Chem.* **1998**, *37*, 4278.